Article:

Bellasio, C., Quirk, J. orcid.org/0000-0002-0625-8323, Buckley, T.N. et al. (1 more author) (2017) A dynamic hydro-mechanical and biochemical model of stomatal conductance for C4 photosynthesis. Plant physiology, 174 (3). ISSN 0032-0889

https://doi.org/10.1104/pp.17.00666

A dynamic hydro-mechanical and biochemical model of stomatal conductance for C_4 photosynthesis

Chandra Bellasio, Joe Quirk, Thomas N. Buckley, and David J. Beerling

Supporting notes

Note S1. Equations to derive a set of key photosynthetic quantities consistent with Eqn 16 in the main paper.

A smoothed value for CO_2 concentration in the BS is given by:

$$C_{\mathrm{BS\,MOD}} = \frac{C_{\mathrm{BS\,(C)}} + C_{\mathrm{BS\,(J)}} - \sqrt{\left(C_{\mathrm{BS\,(C)}} + C_{\mathrm{BS\,(J)}}\right)^2 - 4\theta_A C_{\mathrm{BS\,(C)}} C_{\mathrm{BS\,(J)}}}}{2\theta_A}. \qquad \mathrm{S1}$$

Consistently,

$$V_{\mathrm{C\,MOD}} = \frac{A_{\mathrm{MOD}} + R_{\mathrm{LIGHT}}}{1 - \gamma^* \frac{O_{\mathrm{BS}}}{C_{\mathrm{BS\,MOD}}}}, \qquad \mathrm{S2}$$

where O_{BS} is calculated with Eqn 4.

V_{OMOD} is given by:

$$V_{\mathrm{O\,MOD}} = V_{\mathrm{C\,MOD}}\, 2\, \gamma * \frac{O_{\mathrm{BS}}}{C_{\mathrm{BS\,MOD}}}. \qquad \mathrm{S3}$$

Leakiness is:

$$L_{\mathrm{MOD}} = g_{\mathrm{BS}}(C_{\mathrm{BS\,MOD}} - C_{\mathrm{M}}), \qquad \mathrm{S4}$$

where C_M is calculated through Eqn 17.

Finally,

$$V_{\mathrm{P\,MOD}} = L_{\mathrm{MOD}} + A_{\mathrm{MOD}} + R_{\mathrm{M}}. \qquad \mathrm{S5}$$

Supporting Figures

Figure S1. Responses to incident irradiance (PPFD) of assimilation rate, A (top), and stomatal conductance, g_S (bottom), for three C_4 grasses: Eragrostis curvula (left), Heteropogon contortus (middle) and Themeda triandra (right). Symbols show observed means ± S.E. (n = 8, 5 and 3, respectively) and lines show model simulations.

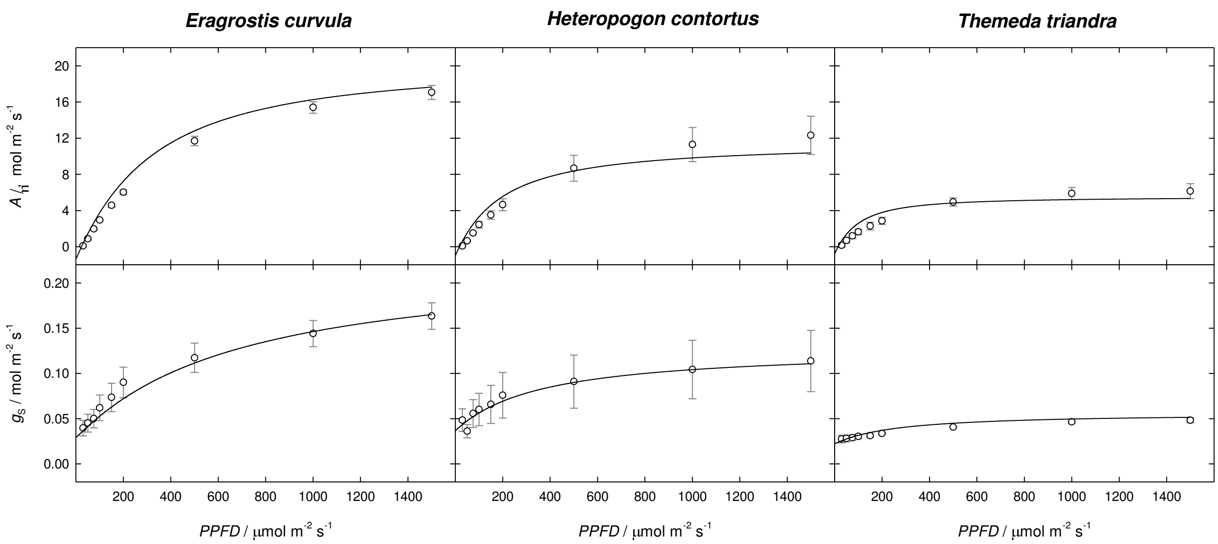

Figure S2. Simulated dynamics of K_{LEAF} in response to PPFD. K_{LEAF} increases from a value of $K_{LEAFMIN}$=20 mmol m^{-2} s^{-1} MPa^{-1} (panel A) or $K_{LEAFMIN}$=10 mmol m^{-2} s^{-1} MPa^{-1} (panel B), with three different induction patterns: an induction in the dark ($K_M(K_{LEAF})$=1 μmol m^{-2} s^{-1}), an induction in moderate light ($K_M(K_{LEAF})$=200 μmol m^{-2} s^{-1}, or an induction in high light ($K_M(K_{LEAF})$=500 μmol m^{-2} s^{-1}).

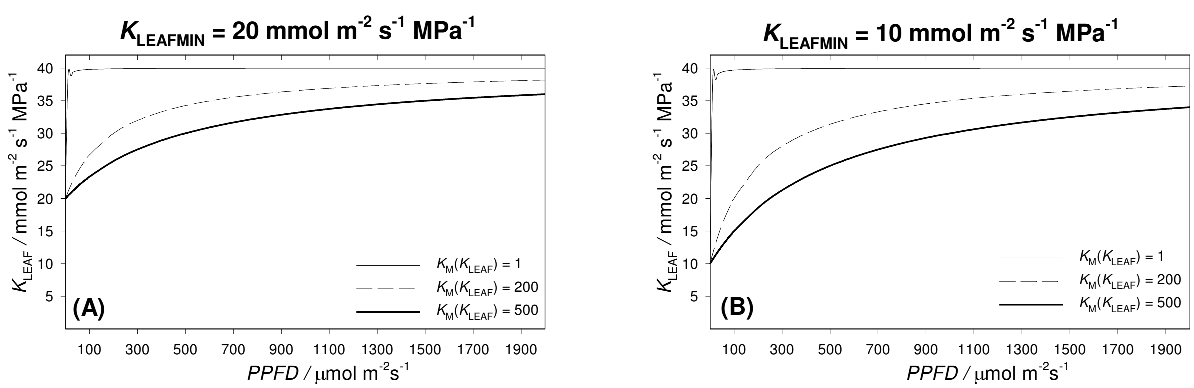

Figure S3. Simulated dynamics of g_S in response to PPFD, when K_{LEAF} is allowed to vary. Three increasingly pronounced patterns were simulated. Panel **A** shows outputs generated for $K_{LEAFMIN}$=20 mmol m^{-2} s^{-1}, D_S=10 mmol H_2O mol air $^{-1}$, Ψ_{Soil}=0 MPa, with three different induction patterns (see Figure S2): $K_M(K_{LEAF})$=1 µmol m^{-2} s^{-1}, $K_M(K_{LEAF})$=200 µmol m^{-2} s^{-1}, or $K_M(K_{LEAF})$=500 µmol m^{-2} s^{-1} (curves from top to bottom). Panel **B** shows outputs generated for $K_{LEAFMIN}$=10 mmol m^{-2} s^{-1} D_S=10 mmol H_2O mol air $^{-1}$, Ψ_{Soil}=0 MPa and the same three $K_M(K_{LEAF})$ described above. Panel **C** shows outputs generated for $K_{LEAFMIN}$=10 mmol m^{-2} s^{-1} D_S=50 mmol H_2O mol air $^{-1}$, Ψ_{Soil}=-1 MPa and the same three $K_M(K_{LEAF})$ described above.

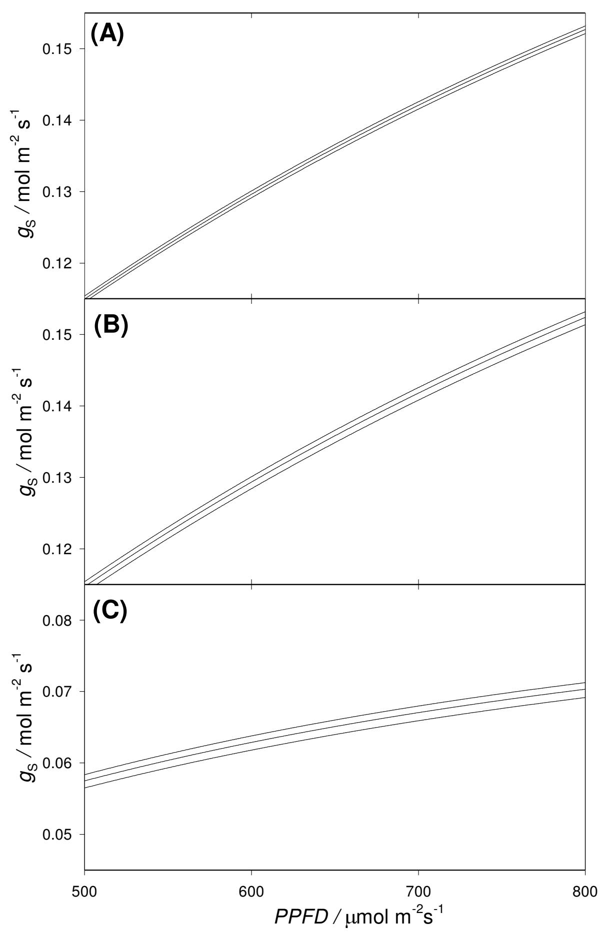

Figure S4. Empirical correction of model inputs V_{CMAX} and J_{ATPMAX} for non-stomatal limitations under decreasing Ψ_{Soil} (Eqn 15).

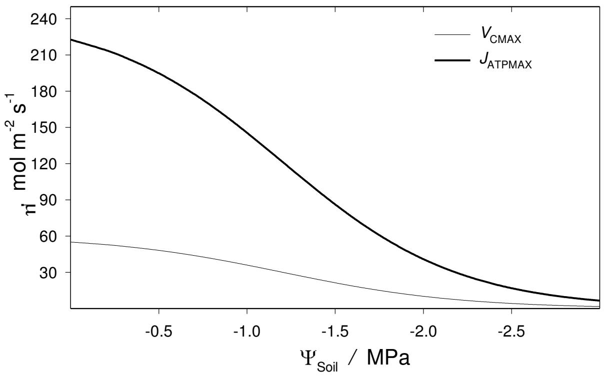

Figure S5. Simulated responses of A and g_S to variable K_{PLANT} at three levels of PPFD. External CO_2 concentration C_a was set at 400 μmol mol^{-1} and D_S at 10 mmol mol^{-1}, for other inputs see Table 1 of the main paper.

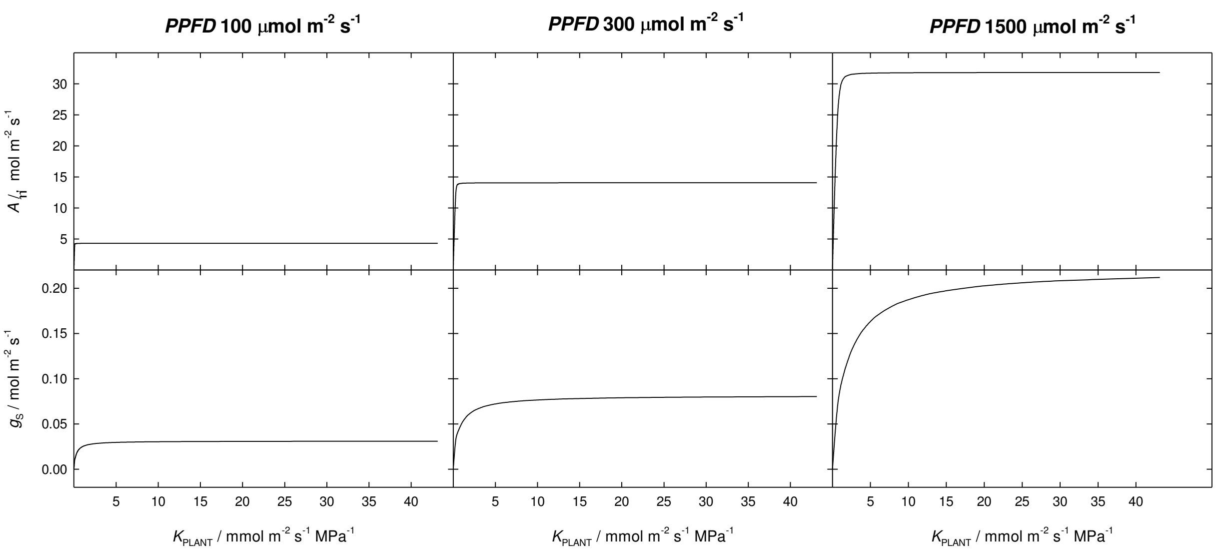

Supporting Tables

Table S1. Additional definitions and units used in Table S2.

Symbol	Definition	Values / Units / source
A_{SAT}	CO_2–saturated *A*, under the PPFD of *A*/*Ci*-curves	µmol m^{-2} s^{-1}
b	*y*-intercept of the *Y(II)*-*Y(CO₂)* linear fit i.e. the fraction of *Y(II)* used by alternative ATP sinks	dimensionless (Valentini et al., 1995)
F	Photorespiration rate, or rate of photorespiratory CO_2 evolution $F = 0.5 \cdot V_O$	µmol m^{-2} s^{-1}
GA	Gross assimilation, GA=A+R_{LIGHT}. Represents the net biochemical CO_2 uptake GA=V_C-F	µmol m^{-2} s^{-1}
GA_{SAT}	Light–saturated *GA*, under the CO_2 concentration of light–curves	µmol m^{-2} s^{-1}
g_{BS}	BS conductance to CO_2 diffusion	mol m^{-2} s^{-1}
J_{ATPSAT}	Light–saturated ATP production rate	µmol m^{-2} s^{-1}
k'	Slope of the linear fit of *Y(II)* against $Y(CO_2)$	dimensionless (Valentini et al., 1995)
LCP	Light compensation point, i.e. *PPFD* when *A*=0. At the *LCP* (V_C=R_{LIGHT}+F).	µmol m^{-2} s^{-1}
$PPFD_{50}$	*PPFD* which half saturates either *GA* or *J*	µmol m^{-2} s^{-1}
R_{LIGHT},	Respiration *in the light*	µmol m^{-2} s^{-1} R_M = ½ R_{LIGHT}
s'	A calibration factor to calculate J_{ATP}	dimensionless (Yin et al., 2004)
V_{CMAX}	CO_2–saturated Rubisco carboxylation rate	65 µmol m^{-2} s^{-1}
$Y(CO_2)_{LL}$	Initial (or max.) quantum yield for CO_2 fixation, i.e. quanta required per CO_2 assimilated	CO_2/Quanta, dimensionless
$Y(II)_{LL}$	Initial Yield of photosystem II *Y(II)* extrapolated to *PPFD*=0	dimensionless
$Y(J_{ATP})_{LL}$	Initial (or max.) quantum yield for ATP production, i.e. conversion efficiency of *PPFD* into J_{ATP}	dimensionless
Γ	C_i–A compensation point, i.e. C_i at which *A*=0 and V_C=R_{LIGHT}+F	µmol mol^{-1}
γ*	Half the reciprocal Rubisco specificity $\gamma^*=0.5/S_{C/O}$	0.000233 (Ubierna et al., 2016)
θ	Curvature of the non–rectangular hyperbola describing the *PPFD* dependence of J_{ATP}	dimensionless
ω	Curvature of the non–rectangular hyperbola describing the C_i dependence of *A*	dimensionless
m	Curvature of the non–rectangular hyperbola describing the *PPFD* dependence of *GA*	dimensionless

Table S2. Output obtained by analysing the primary gas exchange responses of maize plants, n=9. Quantities in bold were used in the simulations. The full dataset is in File S2.

			Ambient O_2		Low O_2		
Quantity	Unit	Method	Mean	S.E.	Mean	S.E.	Source
$\mathbf{R_{LIGHT}}$	µmol m^{-2} s^{-1}	Fluorescence–Light (Yin)	1.65	0.15	1.46	0.14	Gas Exchange
$Y(II)_{LL}$	dimensionless	Quadratic	0.693	0.012	0.660	0.012	Gas Exchange
LCP	µmol m^{-2} s^{-1}	Hyperbola	25.3	2.8	22.0	2.6	Gas Exchange
GA_{SAT}	µmol m^{-2} s^{-1}	Hyperbola	40.7	0.74	40.2	1.1	Gas Exchange
$Y(CO_2)_{LL}$	CO_2/quanta	Hyperbola	0.0669	0.0018	0.0679	0.0014	Gas Exchange
$PPFD_{50}$	µmol m^{-2} s^{-1}	Hyperbola	395	14	384	18	Gas Exchange
m	dimensionless	Hyperbola	0.714	0.029	0.708	0.040	Gas Exchange
CE	mol m^{-2} s^{-1}	Hyperbola	2.13	0.54	4.08	2.0	Gas Exchange
A_{SAT}	µmol m^{-2} s^{-1}	Hyperbola	32.9	0.97	33.5	0.93	Gas Exchange
ω	dimensionless	Hyperbola	0.601	0.10	0.633	0.13	Gas Exchange
Γ	µmol m^{-2} s^{-1}	Hyperbola	1.96	1.24	1.01	0.67	Gas Exchange
s'	CO_2/quanta	Yin	–	–	0.312	0.0036	Gas Exchange
k'	quanta/CO_2	*Valentini*	–	–	8.21	0.30	Gas Exchange
b	dimensionless	*Valentini*	–	–	0.0984	0.015	Gas Exchange
$\mathbf{Y(J_{ATP})_{LL}}$	ATP/quanta	*Valentini*	0.363	0.0062	0.343	0.0051	Gas Exchange
$\mathbf{J_{ATPSAT}}$	µmol m^{-2} s^{-1}	*Valentini*	243	12	–	–	Gas Exchange
θ	dimensionless	*Valentini*	0.583	0.061	–	–	Gas Exchange
$PPFD_{50}$	µmol m^{-2} s^{-1}	*Valentini*	483	39	–	–	Gas Exchange
$\mathbf{g_{BS}}$	mol m^{-2} s^{-1}	J_{ATP} from Valentini	0.00147	1.8×10^{-4}	–	–	Gas Exchange
$\mathbf{V_{PMAX}}$	µmol m^{-2} s^{-1}	Mechanistic	94.9	8.9	–	–	Gas Exchange

Table S3. Input quantities for grasses simulations. J_{ATPMAX}, R_{LIGHT}, V_{PMAX} were obtained by analysis of gas exchange data (the full dataset is in File S2) within the C_3 and C_4 photosynthesis modelling framework of Bellasio et al. (2016) for three C_4 grass species. $\chi\beta$ was obtained by fitting the output of Eqn 10 to the data in figure S1. Mean values (± 1 S.D. in parenthesis). θ was 10^{-4}. All other inputs are the same as for maize and listed in Table 1 of the main paper.

Symbol	Units	*Eragrostis curvula*	*Heteropogon contortus*	*Themeda triandra*
$J_{MAX/SAT}$	µmol m^{-2} s^{-1}	153 (68.6)	35.9 (24.3)	43.5 (8.64)
R_{LIGHT}	>0 µmol m^{-2} s^{-1}	1.37 (0.22)	0.938 (0.066)	0.700 (0.171)
V_{CMAX}	µmol m^{-2} s^{-1}	38.2 (17.2)	8.98 (6.06)	10.9 (2.16)
V_{PMAX}	µmol m^{-2} s^{-1}	36.0 (8.97)	15.3 (0.808)	11.24 (1.85)
g_{S0}	mol m^{-2} s^{-1}	0.0292 (0.012)	0.0367 (0.023)	0.0223 (0.004)
$\chi\beta$	mol air $mmol^{-1}$ ATP s^{-1} MPa^{-1}	0.115	0.07	0.016

References

Bellasio C, Beerling DJ, Griffiths H (2016) Deriving C_4 photosynthetic parameters from combined gas exchange and chlorophyll fluorescence using an Excel tool: theory and practice. Plant, Cell & Environment **39:** 1164-1179

Ubierna N, Gandin A, Boyd RA, Cousins AB (2016) Temperature response of mesophyll conductance in three C4 species calculated with two methods: 18O discrimination and in vitro Vpmax. New Phytologist **214:** 66–80

Valentini R, Epron D, De Angelis P, Matteucci G, Dreyer E (1995) In situ estimation of net CO2 assimilation, photosynthetic electron flow and photorespiration in Turkey oak (Q. cerris L.) leaves: diurnal cycles under different levels of water supply. Plant, Cell & Environment **18:** 631-640

Yin X, Van Oijen M, Schapendonk A (2004) Extension of a biochemical model for the generalized stoichiometry of electron transport limited C3 photosynthesis. Plant, Cell & Environment **27:** 1211-1222